Electronic Supplementary Material (ESI) for New Journal of Chemistry

29 August 2019

Phosphorylated micro- *vs* nano-cellulose: A comparative study on their surface functionalisation, growth of titanium-oxo-phosphate clusters and removal of chemical pollutants

Sara Blilid,[a,b] Nadia Katir,[a] Jamal El Haskouri,[c] Mohamed Lahcini,[b,d] Sébastien Royer,[e] and Abdelkrim El Kadib.[a,*]

[a] *Euromed Research Center, Engineering Division, Euro-Med University of Fes (UEMF), Route de Meknes, Rond-point de Bensouda, 30070, Fès, Morocco.* a.elkadib@ueuromed.org
[b] *Laboratory of Organometallic and Macromolecular Chemistry-Composites Materials, Faculty of Sciences and Technologies, Cadi Ayyad University, Avenue Abdelkrim Elkhattabi, B.P. 549, 40000 Marrakech, Morocco*
[c] *Instituto de Ciènci de los Materials de la Universidad de Valencia, Calle catedratico José Beltran, 2 CP 46980 Paterna Valencia, Spain*
[d] *Mohammed VI Polytechnic University, Lot 660, Hay Moulay Rachid, 43150 Ben Guerir, Morocco.*
[e] *Univ. Lille, CNRS, ENSCL, Centrale Lille, Univ Artois, UMR 8181 – UCCS – Unité de Catalyse et Chimie du Solide, F-59000 Lille, France*

Experimental section.

Materials Commercially available reagents ($POCl_3$, $P_3N_3Cl_6$, $Ti(OiPr)_4$ and $Ti(OiPr)_2(acac)_2$ and solvents were purchased from Across and Sigma-Aldrich and used without further purification. Microcristalline cellulose (**MCC**, CAS 9004-34-6) was purchased from Sigma-Aldrich.

General ^{13}C and ^{31}P CP MAS NMR spectra were acquired on a Bruker Avance 400 WB spectrometer operating at 100 MHz and 162 MHz respectively under cross-polarization conditions. Fourier transformed infrared (FTIR) spectra were obtained with a Perkin-Elmer Spectrum 100FT-IR spectrometer on neat samples (ATR FT-IR) using 16 scans. DRUV spectra were measured in the 200–800 nm range using spectral on as the reference on a Perkin-Elmer Lambda 1050 spectrometer equipped with an integrating sphere (Lapshere, North Sutton, USA). The XPS measurements were performed on a Versa Probe-II tool from ULVAC-Phi using a focused monochromated Al Ka radiation (1486.6 eV). The spectrometer was calibrated using the photoemission lines of gold (Au 4f7/2 emission at 83.9 eV, with reference to the Fermi level). The core level peaks and the survey spectra were recorded with a constant pass energy of 23.3 eV and 117.9 eV, respectively. All spectra were recorded using electron and argon charge neutralizer guns to minimize the surface charging effect that may occur at the insulating powder surface during the photoemission process. All spectra were calibrated using the contamination carbon C 1s emission at 284.8 eV. The XPS spectra were fitted using Multipak V9.1 software in which a Shirley background was assumed, and the peak fittings of the experimental spectra were defined by a combination of Gaussian (80%) and Lorentzian (20%) distributions. Thermogravimetric analyses (TGA) were performed on a Q500 (TA instrument) using a heating rate of 10 °C/min from room temperature to 700 °C under air. Scanning electronic microscopy (SEM) images were obtained using a JEOL JSM 6700F. For electron microscopy analyses, the samples were dispersed in ethanol and placed onto a carbon coated copper microgrid and left to dry before observation. The TEM and HRTEM microstructural characterizations were carried out using a JEOL JEM-1010 instrument operating at 100 kV and equipped with a CCD camera and a Tecnai G2 F20(FI) instrument, respectively. Powder X-ray diffraction (XRD) was carried out using a Bruker D8 Advance diffractometer with monochromatic Cu Ka source operated at 40 kV and 40 mA. Patterns were collected in steps of 0.02 (2a) over the angular range 1–10.0 (2θ), with an acquisition time of 25 s per step. Additionally, XRD patterns were recorded over a wider angular range, 10–80, (2θ) to determine the presence of crystalline phases. Nitrogen adsorption-desorption isotherms were recorded in an automated Micromeritics ASAP2020 instrument. Prior to the adsorption measurements, the samples were outgassed in situ in vacuum (106 Torr) at 120 C for 15 h to remove adsorbed gase.

Preparation of CNC. Cellulose nanocrystals (**CNC**) were prepared by H_2SO_4 hydrolysis of cotton wool (purchased from Fisher Scientific). Acid hydrolysis was performed at 45 °C with 65 wt% H_2SO_4 for 60 min under mechanical stirring. The resulting suspension was washed with water by using successive centrifugations at 10,000 rpm for 20 min each step. Dried **CNC** powder was obtained by freeze-drying process.*

*Stephanie Beck-Candanedo, Maren Roman and Derek G. Gray. *Biomacromolecules*. 2005, 6, (2). 1048-1054.

Synthesis of phosphorylated cellulose P-MCC and P-CNC. In a typical procedure using $POCl_3$ as the phosphorylating agent, 1mL (1.06 mmol) of $POCl_3$ was dropped into the suspension of 200 mg of **MCC** or **CNC** in 5 mL of THF (stirred for 10 min) and the resulting solution was stirred at room temperature for 24 hours. Then 10 mL deionized water were added to the mixture and kept under stirring for 1 hours. Finally, the product was collected through centrifugation and was dried at 60 °C for 24 h.

Synthesis of phosphorylated cellulose PN-MCC and PN-CNC. In a typical procedure using hexachlorocyclotriphosphazene ($N_3P_3Cl_6$) as the phosphorylating agent, 100 mg (0.29 mmol) of $N_3P_3Cl_6$ were added to a suspension of 100 mg of **MCC** or **CNC** in 5 mL of THF (stirred for 10 min) and the resulting mixture was stirred at room temperature for 24 hours. Then 10 mL deionized water was added to the mixture and kept under stirring for 1 hours. Finally, the product was collected through centrifugation and was dried at 60 °C for 24 h.

Synthesis of TiO_2@MCC and TiO_2@CNC. For typical procedure for grafting, 0.54 mL (1.82 mmol) of $Ti(OiPr)_4$ was added to a suspension of 100 mg of **MCC** or **CNC** in 5 mL of THF and the resulting mixture was stirred at room temperature for 24 hours. After centrifugation and extensive washing of the precipitate with THF, the collected solids were dried at 60 °C for 24 hours

Synthesis of TiO_2@P-MCC and TiO_2@P-CNC. For typical procedure for post-grafting, 0.54 mL (1.82 mmol) of $Ti(OiPr)_4$ was added to a suspension of 100 mg of **P-MCC** or **P-CNC** in 10 mL of THF and the resulting mixture was stirred at room temperature for 24 hours. After centrifugation and extensive washing of the precipitate with THF, the collected solids were dried at 60 °C for 24 hours.

Synthesis of Ti_{acac}-O-P@MCC and Ti_{acac}-O-P@CNC. For typical procedure for insitu method,. 0.5 mL (0.53 mmol) of $POCl_3$ was added to a solution of 1.33 mL (2.72 mmol) of $Ti(OiPr)_2(acac)_2$ in 10 mL of THF. The solution was stirred at room temperature for 8hours. Then 2 mL were added and the mixture was stirred at room temperature. After 24 hours, this mixture was added to a suspension of 100 mg of **MCC** or **CNC** in 10 mL of THF. The new solution was stirred 24 hours at room temperature. Finally, the product was collected through centrifugation and was dried at 60 °C for 24 h.

Dye removal. To a volume of 10 mL of an aqueous solution of Congo Red (50 $mg.L^{-1}$), 10 mg of the selected adsorbent (either **MCC**, **CNC** or their phosphorylated derivatives) was added. The mixture was kept under magnetic stirring for 4 hours (equilibrium time). A significant change from red to violet was frequently observed during **P-MCC** and **P-CNC** adsorption, witnessing on the strong interaction between the solid and the dye. After filtration, the resulting solution was analyzed by UV-vis spectroscopy to determine the remaining dye concentration.

S1. Characterization data of MCC and CNC

S1a. Characterization data of MCC

DRIFT analysis

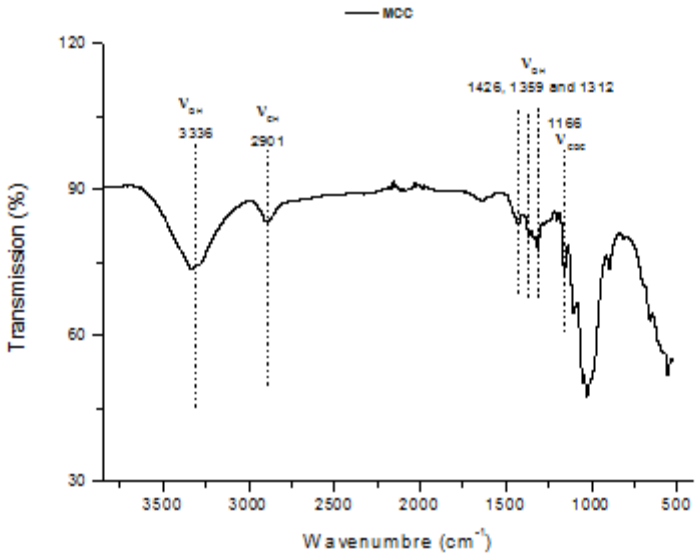

Solid-state MAS ^{13}C NMR

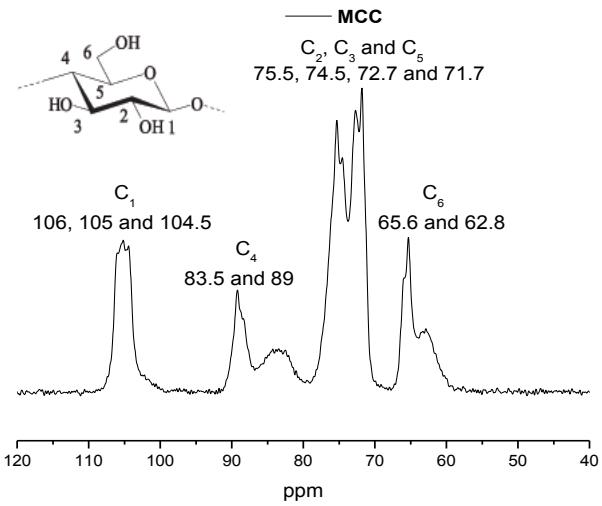

XRD of MCC

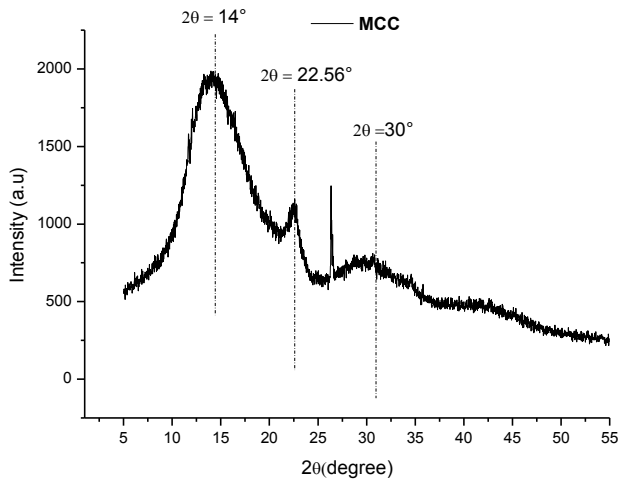

SEM of MCC

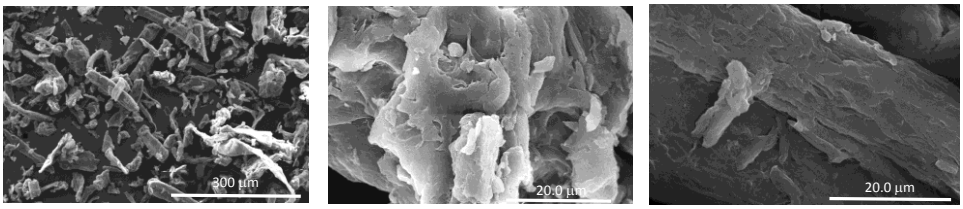

TEM of MCC

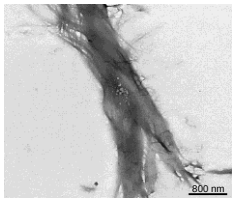

S1b. Characterization data of CNC

DRIFT analysis

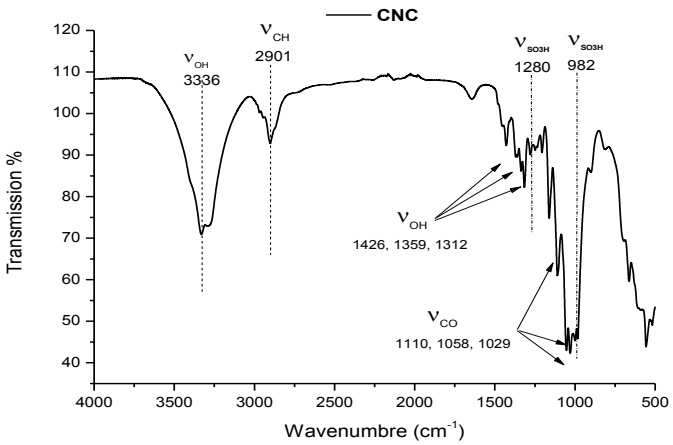

Solid-state MAS ^{13}C NMR

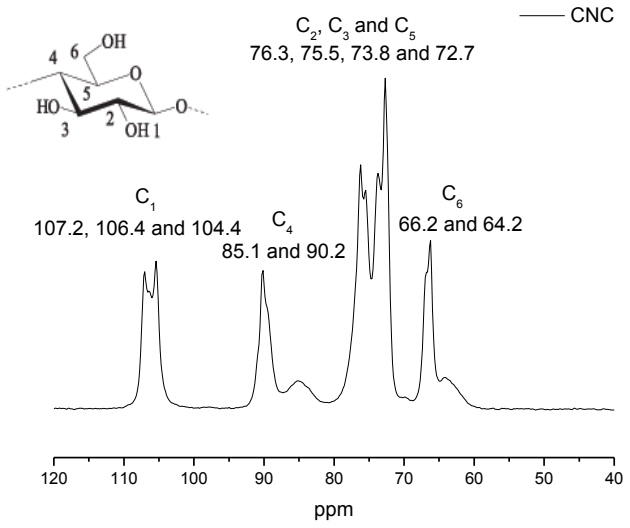

XRD of CNC

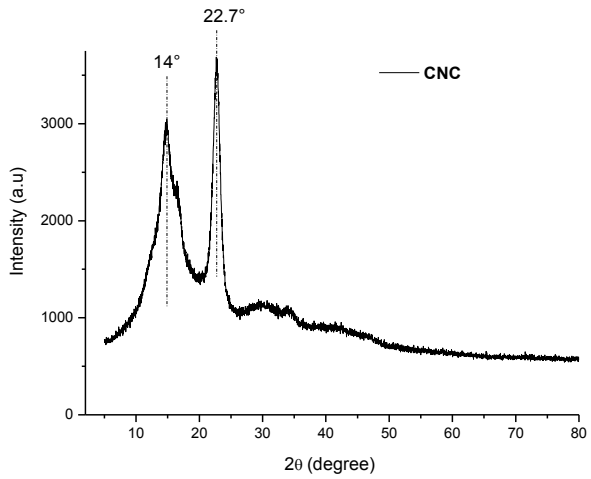

SEM and TEM of CNC

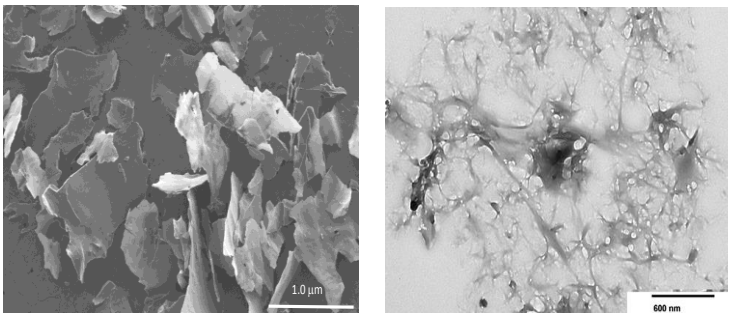

TGA of CNC versus MCC

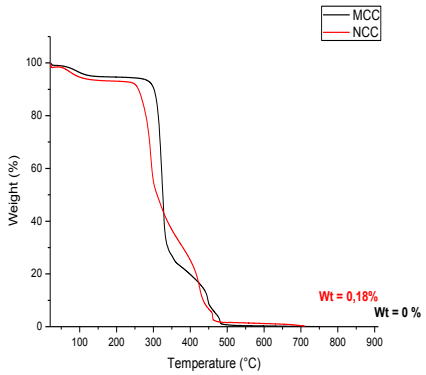

S2. DRIFT analyses of P-MCC and P-CNC

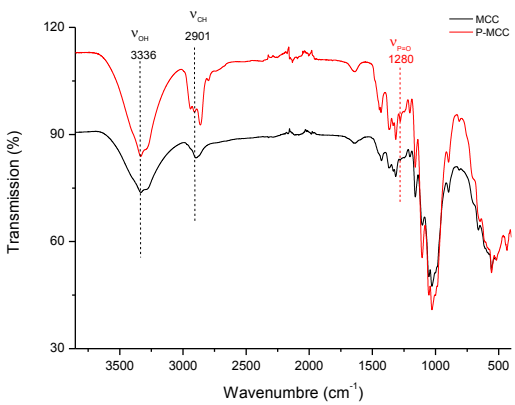

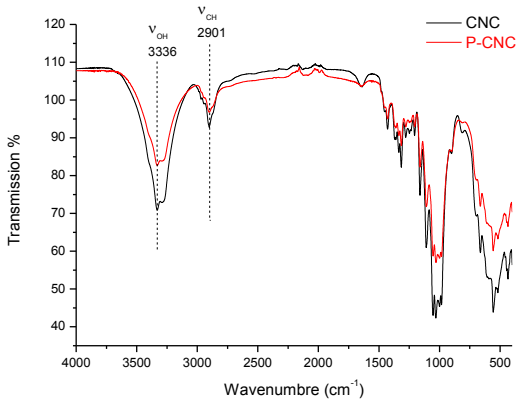

S3. ^{13}C CP MAS NMR of P-MCC, NP-MCC, P-CNC and PN-CNC

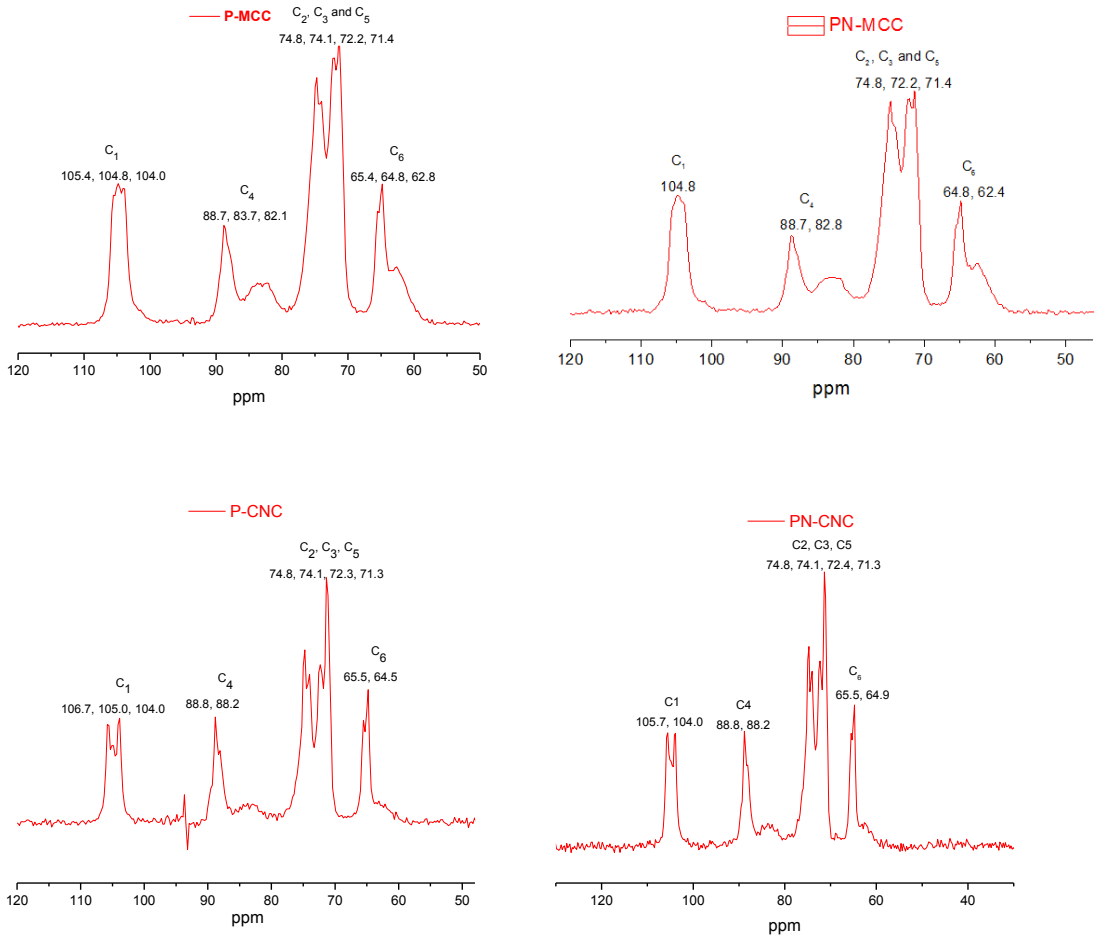

S4. XPS analyses of P-MCC, NP-MCC, P-CNC and NP-CNC

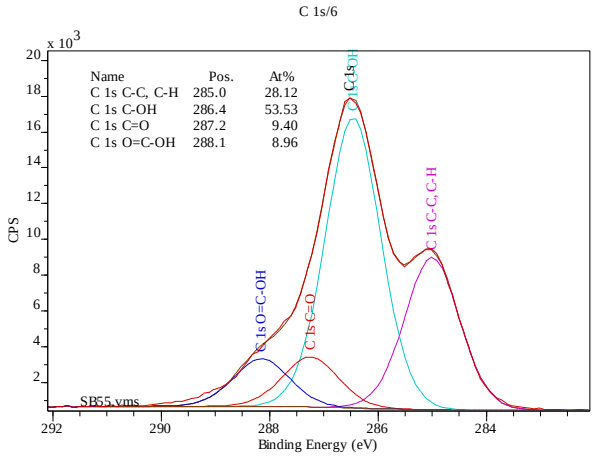

P-CNC

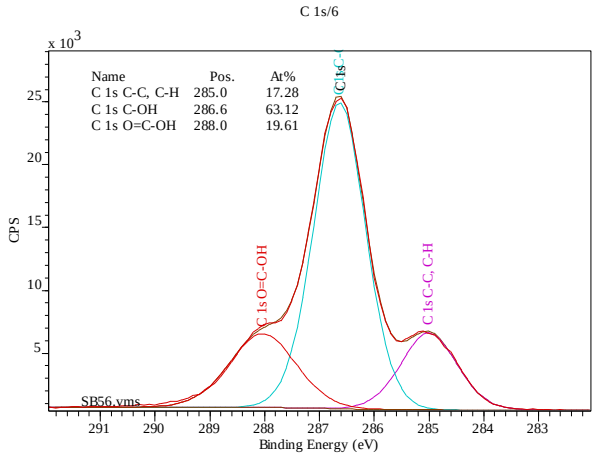

PN-CNC

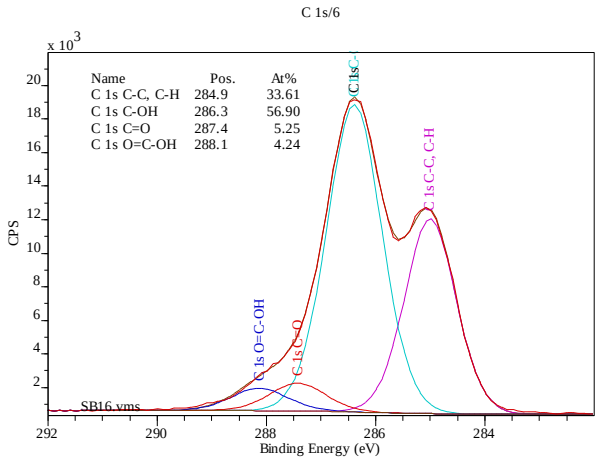

P-MCC

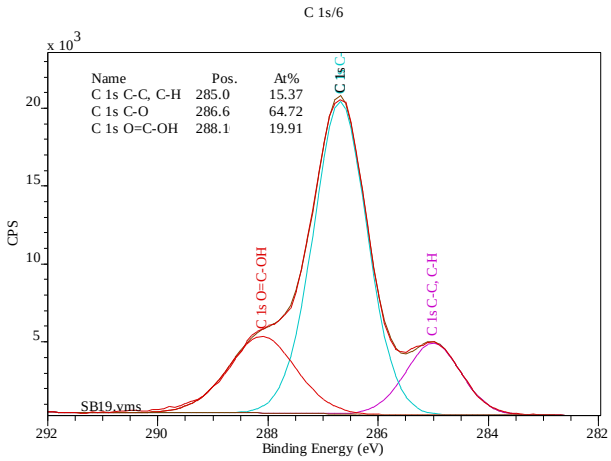

PN-MCC

	Atomic concentration (%)				Binding energy (eV)		
	C	**O**	**P**	**Cl**	**C 1s**	**O 1s**	**P 2p**
P-MCC	70.8	26.1	1.2	1.9	286.4	532.7	134.5
P-CNC	63.3	33.7	2.3	0.1	286.5	532.8	134.5
PN-MCC	60.8	38.8	0.2	0.2	286.7	533.0	134.2
PN-CNC	58.1	39.7	1.3	0.2	286.6	533.0	134.4

Another diverging pattern is the noticeable discrepancy in the amount of persistent chloride in **MCC** and **CNC**, under anhydrous conditions. High amount of entrapped Cl derivatives corresponding probably to non-hydrolysed P-Cl species was found in **MCC** compared to **CNC**. Theoretical Cl-to-P value for the starting material is 3. XPS studies show a ratio of 1.58 for **P-MCC** and 1.00 for **NP-MCC**, corresponding to an advanced hydrolysis extent of 48% and 67%, respectively. Comparatively, a nearly complete hydrolysis occurred within **CNC**, reaching an advanced hydrolysis extent of 98% for **P-CNC** and 95% for **PN-MCC**. A reasonable explanation could be the entanglement of chlorine motifs within the amorphous regions of **MCC**, making P-Cl hydrolysis and/or removal of chlorine from the network more difficult in **MCC** compared to the well-exposed surface in **CNC**. The presence in **CNC** of ester sulphate groups that can be expulsed from the surface under nucleophilic action of chlorine (through formation of Cl-SO_3H) could be another reason of scavenging chlorine from the surface. In support to this assumption, sulphate ester removal from **CNC** is routinely performed by treating cellulose nanocrystals under acidic conditions; the use of $POCl_3$ in our experiments induces a decrease of the pH of the milieu from nearly neutral pH of ~ 5 to almost highly acidic one (pH ~ 1).

S5. Nitrogen adsorption-desorption isotherm profile of MCC, TiO_2@P-MCC and Ti_{acac}-O@MCC

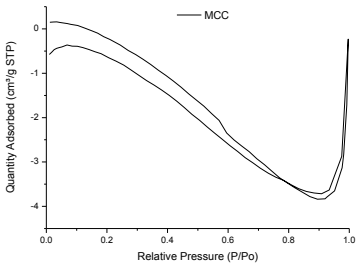

BET Surface Area: 0 m²/g

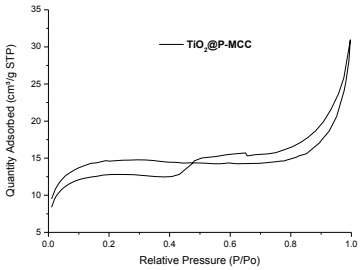

BET Surface Area: 51 m²/g
Pore diameter: 10.28 nm
volume of pores: 30.94 cm³/g

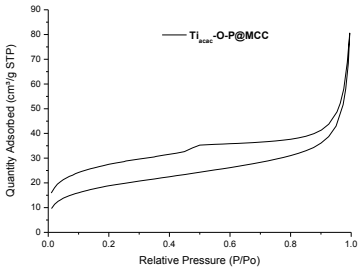

BET Surface Area: 68 m²/g
Pore diameter 8.48 nm
volume of pores: 68.35 cm³/g

S6. EDX analyses

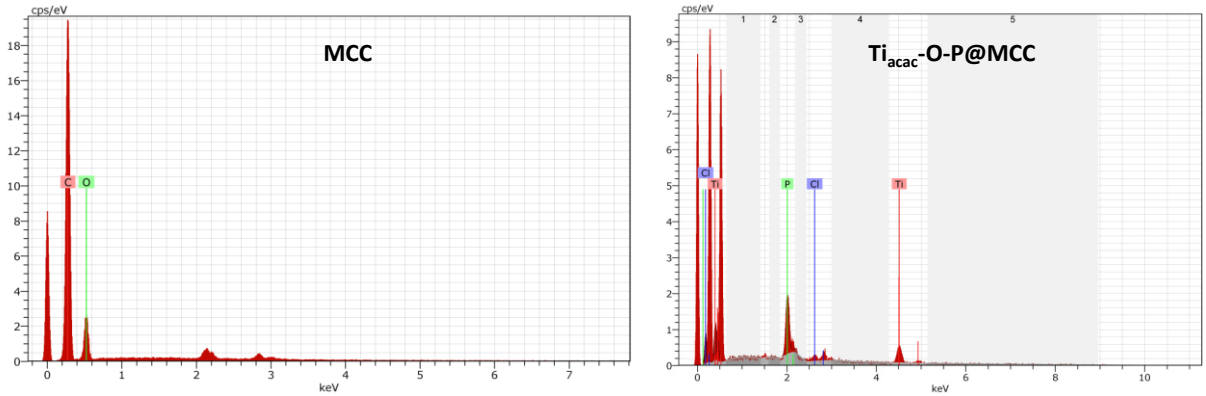

EDX analysis shows the presence of Ti, P and Cl in the isolated material. Mapping in different regions reveals similar ratio of P, Ti and C inside.

Zoom on the HRTEM provided in Figure 6 to show clearly the presence of discrete crystalline titanium dioxide clusters.

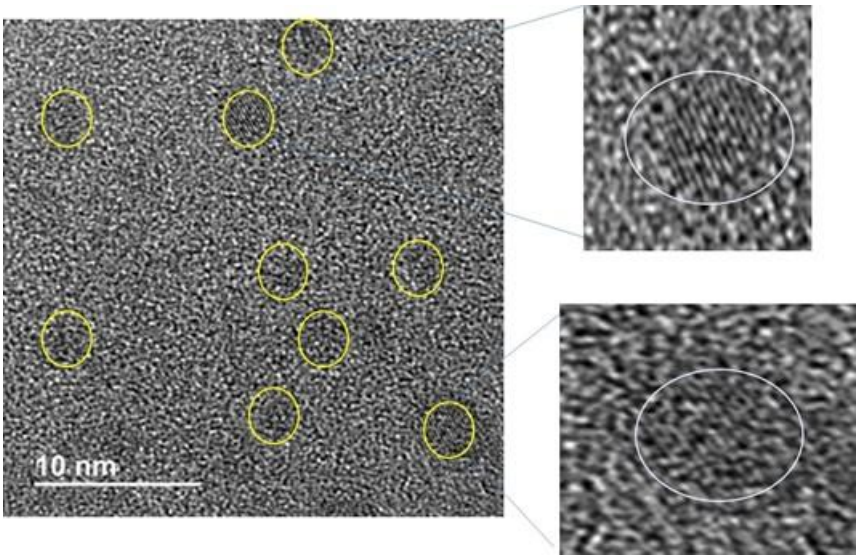

S7. DRIFT analyses of TiO_2@P-MCC, Ti_{acac}-O-P@MCC and Ti_{acac}-O-P@CNC (plotted against the starting supports).

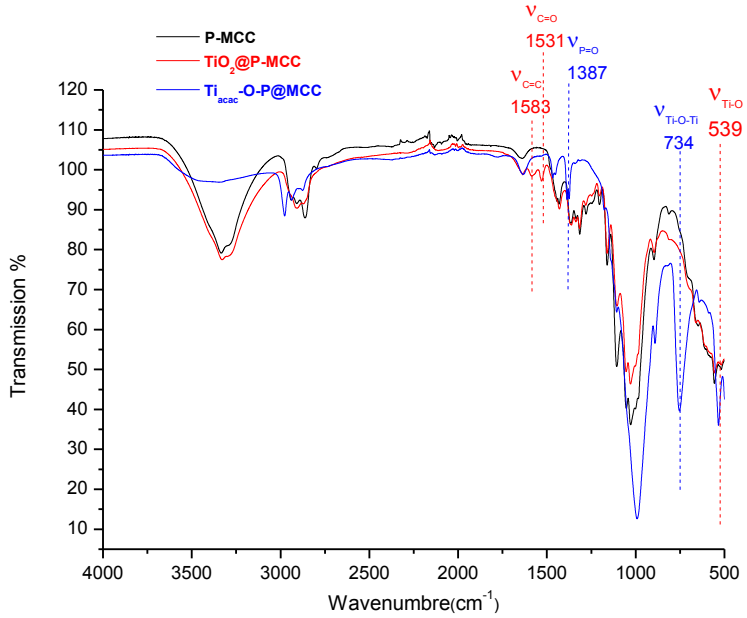

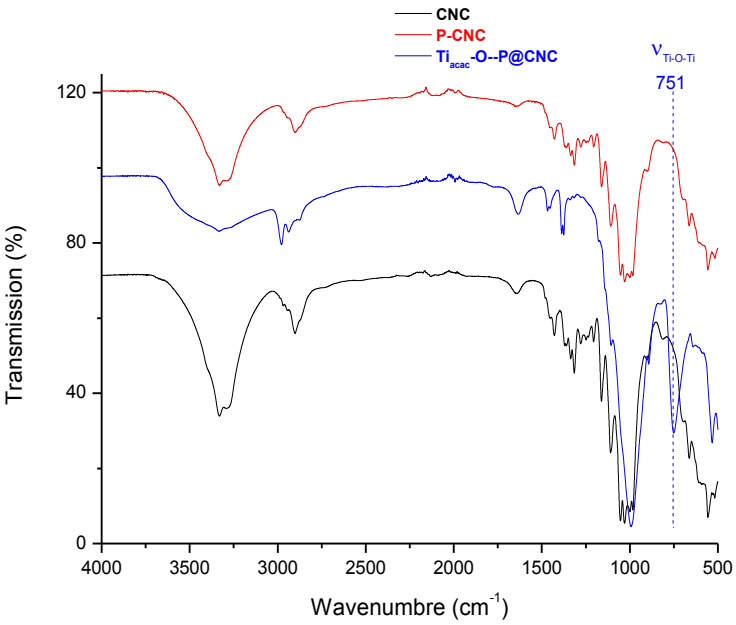

Besides the signature of phosphorus in DRIFT, the presence of additional bands at 540, 750 and between 900 and 1000 cm^{-1} confirms the growth of titanium-oxo- clusters inside.

S8. XRD analyses of TiO_2@MCC, TiO_2@P-MCC, Ti_{acac}-O-P@MCC, TiO_2@CNC and Ti_{acac}-O-P@CNC

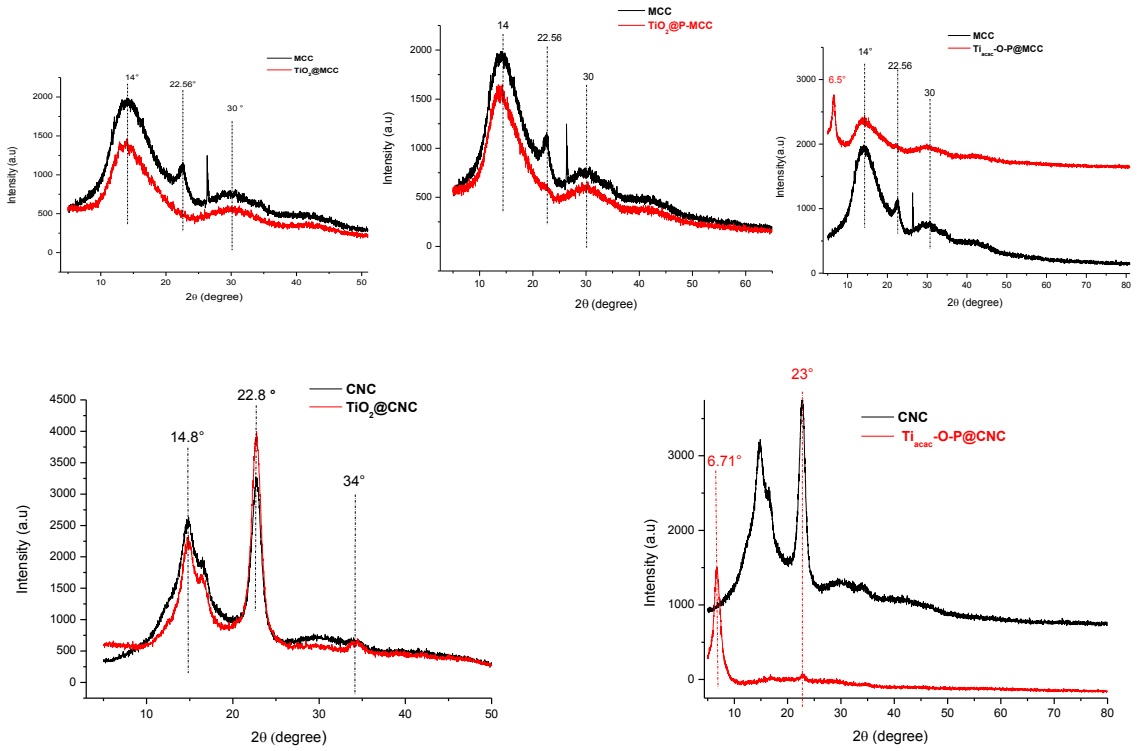

S9. TGA analyses of MCC, Ti-O-P@MCC and Ti_{acac}-O-P@MCC

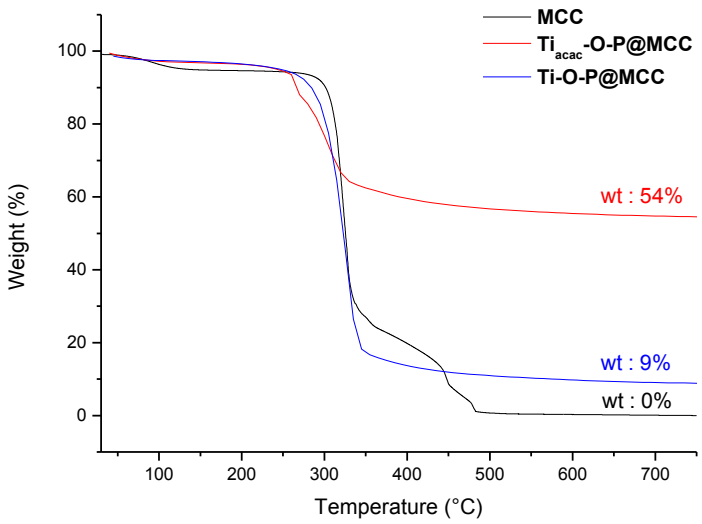

S10. Photos of the waste-water solution after adsorption

Photos of Congo red water aqueous solutions depending on the material used

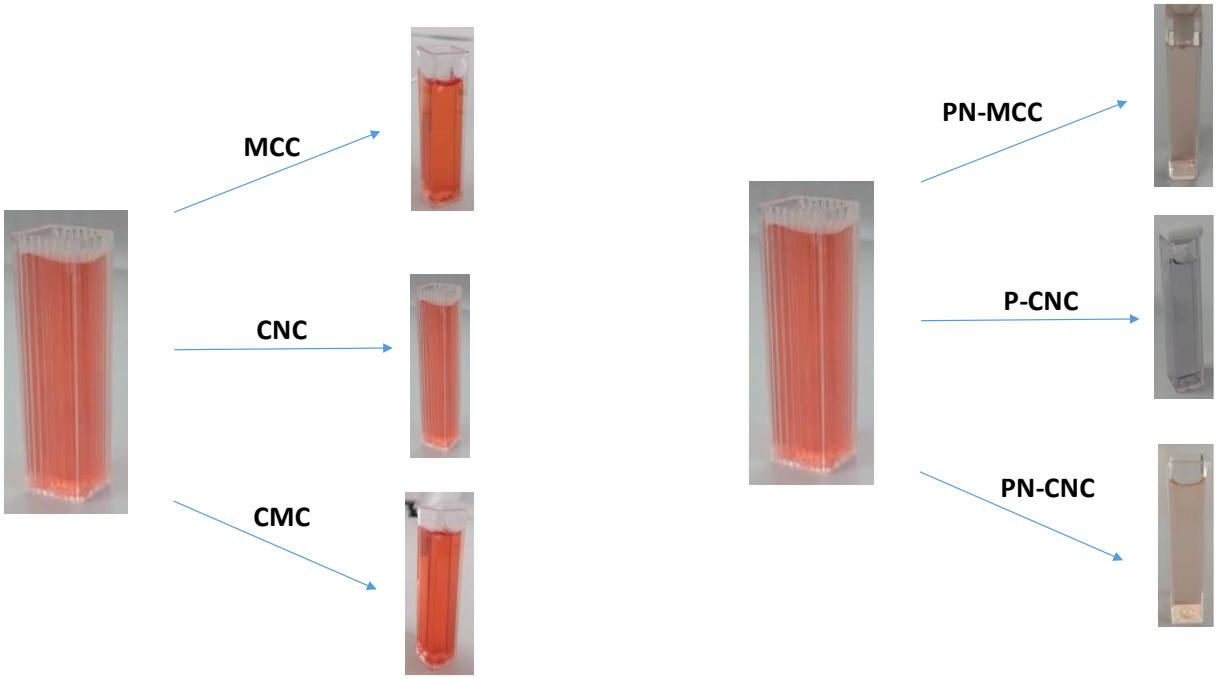

Photos of Malachite green water aqueous solutions depending on the material used